Charm dijet angular distributions in γp collisions with ZEUS at HERA

Leonid Gladilin *
(on behalf of the ZEUS Collaboration)
DESY, ZEUS experiment, Notkestr. 85, 22607 Hamburg, Germany
E-mail: gladilin@mail.desy.de

Dijet angular distributions of photoproduction events in which a $D^{*\pm}$ meson is produced in association with one of two energetic jets have been measured using an integrated luminosity of $120\,\mathrm{pb}^{-1}$. The results are compared with predictions from leading-order parton-shower Monte Carlo models and with next-to-leading-order QCD calculations.

1 Introduction

In photoproduction processes at HERA, a quasi-real photon with virtuality $Q^2 \sim 0$ is emitted by the incoming electron and interacts with the proton. At leading order (LO) in QCD, two types of processes are responsible for the production of heavy quarks: the direct photon processes, where the photon participates as a point-like particle, and the resolved photon processes, where the photon acts as a source of partons. In the direct photon-gluon-fusion (PGF) process (Fig. 1a), the entire photon momentum is involved and the propagator is a spin-$\frac{1}{2}$ quark propagator. In resolved photon processes, a parton from the photon scatters off a parton from the proton (Figs. 1b, 1c and 1d), and only a fraction of the photon momentum participates in the hard scatter. Charm quarks present in the parton distributions of the photon, as well as of the proton, lead to processes like $cg \rightarrow cg$, which are called charm-excitation processes (Figs. 1c and 1d). The dominant t-channel charm-excitation diagram has a spin-1 gluon propagator (Fig. 1d). At next-to-leading order (NLO) in QCD, only the sum of direct and resolved processes is unambiguously defined.

To identify contributions of different charm-production processes and to verify relevant QCD calculations, photoproduction of events with a $D^{*\pm}$ meson and at least two energetic jets has been studied [1, 2].

*On leave from Moscow State University, supported by the U.S.-Israel BSF

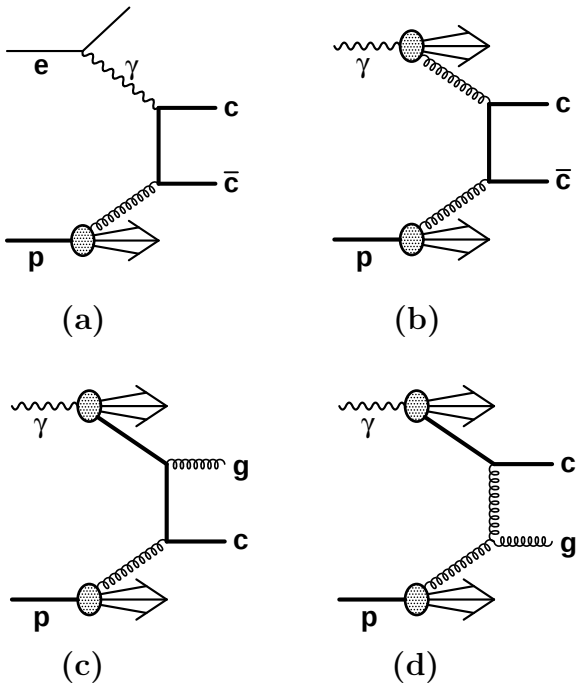

Figure 1: LO QCD charm-production diagrams: (a) direct photon: $\gamma g \rightarrow c\bar{c}$; (b) resolved photon: $gg \rightarrow c\bar{c}$; (c) resolved-photon charm excitation: $cg \rightarrow cg$ (u-channel); (d) resolved-photon charm excitation: $cg \rightarrow cg$ (t-channel).

2 QCD calculations of charm photoproduction

The Monte Carlo (MC) programs PYTHIA [3] and HERWIG [4] simulate heavy-quark photoproduction in the framework of the collinear approach using the on-shell LO matrix elements for direct and resolved photon processes (including charm excitation). Higher-order QCD effects are simulated in the leading-logarithmic approximation with initial- and final-state radiation obeying DGLAP evolution.

The MC program CASCADE [5] simulates heavy-quark photoproduction in the framework of the semi-hard or k_t-factorisation approach using the off-shell

LO PGF matrix element. The resolved photon processes are reproduced by the initial-state radiation based on CCFM evolution.

The NLO QCD calculations of differential cross sections for photoproduction of charm dijet events are available [6] in the fixed-order scheme assuming no explicit charm-excitation component. Charm photoproduction cross sections are calculated in the framework of the collinear approach using the on-shell matrix elements.

3 Dijet angular distributions in photoproduction of charm

An experimental separation of the direct and resolved processes was obtained by a selection on the variable

$$x_\gamma^{\rm obs} = \frac{E_T^{\rm jet1}\eta^{\rm jet1} + E_T^{\rm jet2}\eta^{\rm jet2}}{2yE_e},$$

where yE_e is the initial photon energy. The variable $x_\gamma^{\rm obs}$ is the fraction of the photon's momentum contributing to the production of the two jets. The measured $D^{*\pm}$ photoproduction cross section peaks at $x_\gamma^{\rm obs} \sim 1$, in agreement with the expectation for direct photon processes. A large cross section is also measured at low $x_\gamma^{\rm obs}$, where resolved processes are expected to contribute significantly. The selection of $x_\gamma^{\rm obs} > 0.75$ and $x_\gamma^{\rm obs} < 0.75$ was used to obtain samples enriched in direct and resolved photon processes, respectively.

Sensitivity to the spin of the propagator in the hard subprocess was obtained by measuring the angle between the jet-jet axis and the beam axis in the dijet rest frame. This angle, θ^*, was reconstructed using

$$\cos\theta^* = \tanh\left(\frac{\eta^{\rm jet1} - \eta^{\rm jet2}}{2}\right). \quad (1)$$

The angular dependence of the cross section for processes with a spin-1 gluon propagator is approximately $\propto (1 - |\cos\theta^*|)^{-2}$. This cross section rises more steeply with increasing $|\cos\theta^*|$ than that for processes with a spin-$\frac{1}{2}$ quark propagator, where the angular dependence is approximately $\propto (1 - |\cos\theta^*|)^{-1}$.

Figure 2 shows the differential cross sections as a function of $|\cos\theta^*|$ for the resolved- and direct-enriched samples. The angular distribution of resolved-enriched events exhibits a more rapid rise towards high values of $|\cos\theta^*|$ than

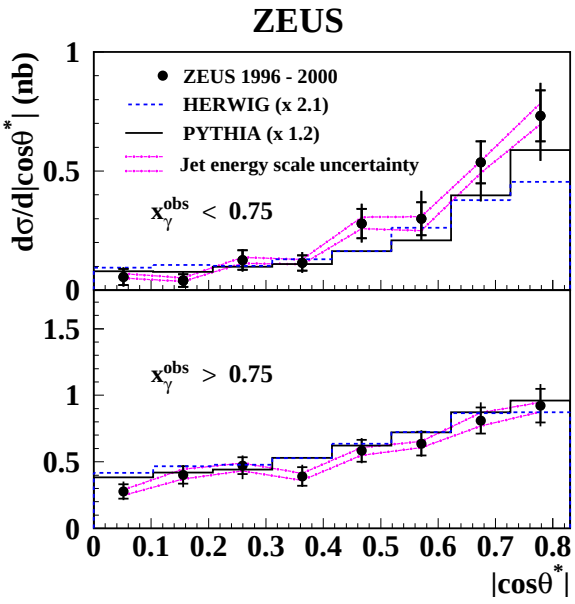

Figure 2: Differential cross-section $d\sigma/d|\cos\theta^*|$ for the data compared with PYTHIA and HERWIG MC simulations. Results are given separately for samples enriched in resolved photon events (upper) and for samples enriched in direct photon events (lower).

does the distribution of direct-enriched events. This observation suggests a large contribution from the t-channel charm-excitation diagram with a spin-1 gluon propagator (Fig. 1d). The data are compared to the PYTHIA and HERWIG predictions normalized to the data. The MC predictions provide adequate descriptions of the shapes of the data distributions.

The two jets can be distinguished by associating the $D^{*\pm}$ meson to the closest jet in $\eta - \phi$ space and calling this jet 1 in Eq. (1). Figure 3 shows the differential cross sections as a function of $\cos\theta^*$ for the resolved- and direct-enriched samples. The angular distribution of resolved-enriched events exhibits a large asymmetry with a mild rise towards $\cos\theta^* = 1$ (proton direction) and

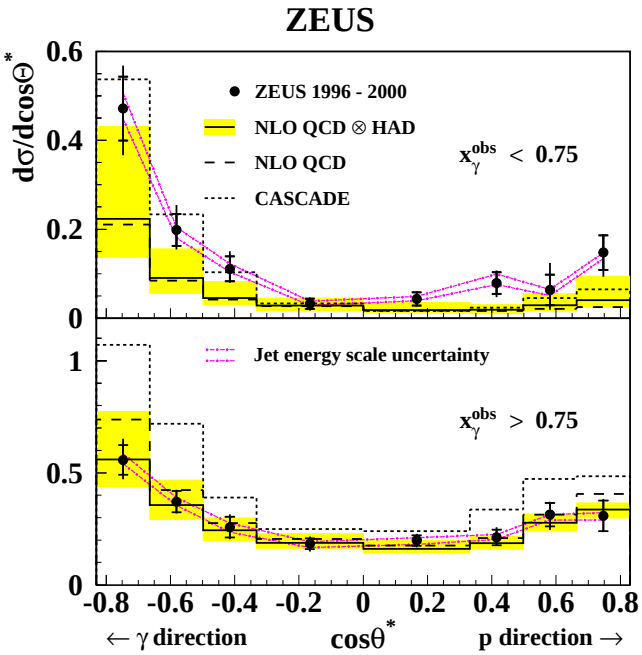

Figure 3: Differential cross-section $d\sigma/d\cos\theta^*$ for the data compared with NLO QCD predictions. Results are given separately for samples enriched in resolved photon events (upper) and for samples enriched in direct photon events (lower).

a strong rise towards $\cos\theta^* = -1$ (photon direction). This observation shows that dijet events with $x_\gamma^{\rm obs} < 0.75$ are dominantly produced by charm quarks coming from the photon side. The $\cos\theta^*$ distribution of direct-enriched events is almost symmetric, as expected for the PGF process. A slight asymmetry can be explained by the feedthrough from resolved photon processes near $\cos\theta^* = -1$ [2].

The CASCADE and NLO predictions are compared to the data in Fig. 3. For $x_\gamma^{\rm obs} < 0.75$, the CASCADE prediction describes the data in the photon direction and underestimates the data in the proton direction. For $x_\gamma^{\rm obs} > 0.75$, the prediction overestimates the data in all regions of $\cos\theta^*$, although the

shape is described reasonably well. The NLO prediction is below the data for $x_\gamma^{\rm obs} < 0.75$ and in agreement with the data for $x_\gamma^{\rm obs} > 0.75$. The shapes are reasonably well described by the NLO predictions.

4 Summary

The measured charm dijet angular distributions show that dijet events at low $x_\gamma^{\rm obs}$ are dominantly produced by charm quarks coming from the photon side. The shapes of the measured distributions are described adequately by the LO collinear calculations (PYTHIA, HERWIG) including a large charm-excitation component.

The shapes of the distributions are reasonably well described by the NLO collinear calculations in the fixed-order scheme assuming no explicit charm-excitation component. The LO k_t-factorisation calculations with the initial-state radiation based on the CCFM evolution (CASCADE) also reproduce the shapes reasonably well. However, the NLO and CASCADE calculations do not reproduce relative contributions of charm dijet events with high and low $x_\gamma^{\rm obs}$ values. The NLO prediction is below the data at low $x_\gamma^{\rm obs}$ and the CASCADE prediction overestimates the data at high $x_\gamma^{\rm obs}$.

References

[1] ZEUS Collaboration, J. Breitweg *et al.*, Eur. Phys. J. **C6** (1999) 67.

[2] ZEUS Collaboration, S. Chekanov *et al.*, Phys. Lett. **B565** (2003) 87.

[3] T. Sjöstrand, Comp. Phys. Comm. **82** (1994) 74.

[4] G. Marchesini *et al.*, Comp. Phys. Comm. **67** (1992) 465.

[5] H. Jung, G. Phys. **G28** (2002) 971.

[6] S. Frixione *et al.*, Nucl. Phys. **B412** (1994) 225;
S. Frixione *et al.*, Nucl. Phys. **B454** (1995) 3;
S. Frixione *et al.*, Phys. Lett. **B348** (1995) 633.